2011 50th IEEE Conference on Decision and Control and
European Control Conference (CDC-ECC)
Orlando, FL, USA, December 12-15, 2011

Control of a Reverse Osmosis Plant by Using a Robust PID Design Based on Multi-objective Optimization

Adrian Gambier, *Senior Member, IEEE*

***Abstract*—Normally, Reverse Osmosis desalination plants (RO plants) include one or two PID (Proportional, Integral, and Derivative) controllers. These controllers usually are not optimally tuned because models are not constant for a long time due to the fact that plant parameters change often. In the current work, the PID controller of the flow rate control loop for permeate is designed by using multi-objective parametric optimization so that the control loop is less sensitive to parameter changes of the plant. Simulation results on a model of a real plant show that the proposed method yields satisfactory performance for wide range of operation conditions.**

I. Introduction

REVERSE osmosis desalination plants use sensible components, which are also prone to parameter changes because membranes are sensitive to temperature of feed water, fouling, scaling and pressure variations. RO plants are normally controlled by using PID control laws, which are tuned but not optimized.

In 1989, the first complex control system, which was based on two pH controllers and an additional pressure controller, was presented in [3]. Model based control has not been intensively used for the control of desalination plants and only few contributions regarding this topic can be found in the literature. Hence, a simple dynamic model was derived for an industrial plant in [4]. DMC (Dynamic Matrix Control) and PID are compared in [21]. Control loops are decoupled in [20] and in [1]. Some ideas of using hybrid control in desalination plants are proposed in [14] and the simultaneous design of two PI controllers for a RO plant by using multi-objective optimization is the subject of [15]. A nonlinear control approach for a high recovery RO system is proposed in [18]. A FTC (Fault Tolerant Control) approach is presented in [17].

Recently, the activities in the field of control of RO plants have been increased. For example in [10], a nonlinear model predictive controller is proposed in order to control a RO plant with feed flow reversal characteristic, an optimization-based control approach is used in [9] for minimizing energy consumption and [5] studies the application of robust control to a tubular RO plant.

A particular control problem with small RO plants consists in that plant parameters change very fast because of fouling and membrane cleaning has to carried out often (e.g. once a week). Thus, process parameters obtained after cleaning are different from the parameters obtained one week later before the next cleaning. Therefore, the control performance deteriorates fast in the course of the week, when the controller was optimal adjusted by using one of these models.

There are basically two approaches in the control engineering literature, which have been designed thinking in the class of problems mentioned above: The adaptive control approach (see e.g. [8]) on one hand, and the robust control approach on the other hand ([23]). However, both control strategies receives a high resistance from plant manufacturers at time that the approach has to be applied in the control praxis. The main reason for that is that the available hardware and software in the RO system were dimensioned for one or two simple control loops and companies rarely agree with introducing a more powerful computational unit. On the contrary, they expect that the control system is not modified in its complexity and structure. Thus, the unique tool for improving the control system performance is the parameter tuning of the PID controllers.

In [16], a procedure for finding the set of all stabilizing PID controllers is proposed but no mechanism for selecting a unique controller is given. In the present work, a methodology based on multiobjective optimization (MOO) is applied to choose a unique set of controller parameters, which shows an acceptable performance and robustness for a wide family of models of a RO plant.

In Section 2, the methodology for the controller design is described. The RO plant and its dynamic characteristic are presented in Section 3. Section 4 is devoted to design the controller for the RO plant. Simulation results are shown and analyzed is Section 5. The last Section 6 is dedicated to present the conclusions.

II. Robust Optimal PID Controller Design

A. PID control law

The classic PID control law is normally given in the form

$$u(s) = K\left[1 + \frac{1}{sT_i} + sT_d\right]e(s), \tag{1}$$

where the controller parameters are the proportional gain K, integral time T_i and derivative time T_d. This law can also be described by the rational function

$$P(s)u(s) = Q(s)e(s), \tag{2}$$

where P and Q are the polynomials

$$P(s) = s \text{ and } Q(s) = q_0 s^2 + q_1 s + q_2. \tag{3}$$

Hence, the coefficients of polynomial $Q(s)$ are defined as

$$q_0 = T_d K, q_1 = K \text{ and } q_2 = K / T_i. \tag{4}$$

This control law is currently used for the control system design based on parameter optimization. However, this control law is practically never used in practice. In [7], it is pointed out that a more convenient description for the PID control law is given by

Manuscript received September 7, 2011.

Adrian Gambier is with the Fraunhofer Institute for Wind Energy and Energy System Technology, Am Seedeich 45, 27572 Bremerhaven, Germany. Phone: +49 471 14290-375; fax: +49 14290-111; e-mail: agambier@ieee.org.

$$u(s) = K\left[b\,r(s) - y(s) + \frac{1}{sT_i}[r(s) - y(s)] - \frac{sT_d}{1 + sT_d / N}\,y(s) \right]. \quad (5)$$

where $0 \le b \le 1$ and $8 \le N \le 20$. Eq. (5) leads to a polynomial description given by

$$P(s)u(s) \;=\; T(s)r(s) - Q(s)y(s)\,, \quad (6)$$

where

$$P(s) \;=\; p_0\,s^2 + p_1\,s + p_2\,, \quad (7)$$

$$T(s) \;=\; t_0\,s^2 + t_1\,s + t_2 \text{ and} \quad (8)$$

$$Q(s) \;=\; q_0\,s^2 + q_1\,s + q_2\,. \quad (9)$$

The coefficients are now

$$p_0 = 1,\; p_1 = N / T_d,\; p_2 = 0\,, \quad (10)$$

$$t_0 = b\,K,\;\; t_1 = K / T_i + b\,K\,N / T_d,\;\; t_2 = K\,N / (T_i\,T_d)\,, \quad (11)$$

$$q_0 = K(N+1),\; q_1 = K / T_i + K\,N / T_d \text{ and } q_2 = K\,N / (T_i\,T_d) \quad (12)$$

Finally, parameters of the PID controller can be calculated back by using the following formulas

$$K = (q_1 p_1 - q_2) / p_1^2,\;\; b = t_0 / K,\;\; T_i = K\;p_1 / q_2 \quad (13)$$

$$N = q_0 / K - 1 \text{ and } T_d = N / p_1 \quad (14)$$

It is important to remark here that this simple change in the control law that includes an additional parameter (p_1) leads to a more complicated optimization problem as it will be described later.

B. Closed loop transfer functions

If the process is now modeled by

$$A(s)y(s) = B(s)\,u(s) \quad (15)$$

and the control error is defined as $e(s) = r(s) - y(s)$, then the closed loop transfer function from r(s) to $e(s)$ and to $u(s)$ are

$$\frac{e(s)}{r(s)} = \frac{\left[A(s)P(s) + [Q(s) - T(s)]B(s)\right]}{A(s)P(s) \;+\; B(s)Q(s)} \quad (16)$$

and

$$\frac{u(s)}{r(s)} = \frac{A(s)T(s)}{A(s)P(s) \;+\; B(s)Q(s)}\,, \quad (17)$$

respectively. Both equations are necessary for solving the optimization problem.

C. Controller design

The controller design follows the steps proposed in [13] for the performance index constituted by the *Integral of the Square Time-weighted Square Error* (ISTSE) and *Control* (ISTSC), which is defined by

$$J = J_e + \lambda J_u\,, \quad (18)$$

with

$$J_e = \int_0^\infty t^2\; e^2(t)\,dt = \frac{1}{2\pi j}\int_{-j\infty}^{j\infty}\left(\frac{-de(s)}{ds}\right)\left(\frac{-de(-s)}{ds}\right)ds\,, \quad (19)$$

$$J_u = \int_0^\infty t^2\; \dot{u}^2(t)\,dt = \frac{1}{2\pi j}\int_{-j\infty}^{j\infty} -s^2\left(\frac{-du(s)}{ds}\right)\left(\frac{-du(-s)}{ds}\right)ds \quad (20)$$

λ is a free weighting parameter used to limit the amplitude of the control signals. The model of the process be now defined as interval polynomials denoted by

$$A^{\#}(s)y(s) = B^{\#}(s)\,u(s) \quad (21)$$

where the polynomials $A^{\#}(s)$ and $B^{\#}(s)$ are given by

$$B^{\#}(s) = s^m + [b_{1,lo}, b_{1,up}]s^{m-1} + \cdots + [b_{m,lo}, b_{m,up}] \quad (22)$$

and

$$A^{\#}(s) = s^n + [a_{1,lo}, a_{1,up}]s^{n-1} + \cdots + [a_{n,lo}, a_{n,up}]\,. \quad (23)$$

with $m < n$. Thus, the PID controller is obtained by using the lower and upper polynomials. This leads to two set of equations, which are formally identical but distinguished by subindices *lo* and *up*. Hence, only one set of equations is presented in the following under the subindex *ind*, which means, given the case, either *lo* or *up*.

$$B_{ind}(s) = s^{n_b} + b_{1,ind}s^{n_b - 1} + \cdots + b_{m,ind} \text{ and} \quad (24)$$

$$A_{ind}(s) = s^{n_a} + a_{1,ind}s^{n_a - 1} + \cdots + a_{n,ind}\,, \quad (25)$$

and the joint optimization of the performances indices

$$J_{ind} = J_{e,ind} + \lambda J_{u,ind}\,, \quad (26)$$

where *ind* means *lo* or *up*, respectively. For J_{ind}, one has

$$J_{e,ind} = \frac{1}{2\pi j}\int_{-j\infty}^{j\infty}\left(\frac{-de_{ind}(s)}{ds}\right)\left(\frac{-de_{ind}(-s)}{ds}\right)ds \quad (27)$$

with

$$e_{ind}(s) = \frac{\left[A_{ind}(s)P(s) + [Q(s) - T(s)]B_{ind}(s)\right]}{A_{ind}(s)P(s) \;+\; B_{ind}(s)Q(s)}\,r(s) \text{ and} \quad (28)$$

$$J_{u,ind} = \frac{1}{2\pi j}\int_{-j\infty}^{j\infty} -s^2\left(\frac{-du_{ind}(s)}{ds}\right)\left(\frac{-du_{ind}(-s)}{ds}\right)ds \quad (29)$$

where

$$u_{ind}(s) = \frac{A_{ind}(s)T(s)}{A_{ind}(s)P(s) \;+\; B_{ind}(s)Q(s)}\,r(s)\,. \quad (30)$$

Coefficients of polynomials $P(s)$, $T(s)$, and $Q(s)$ are obtained solving the multi-objective optimization problem defined by (J_{lo}, J_{up}) taking into account the four Kharitonov's polynomials as constraints in order to guarantee the stability of the closed loop system. The numerical evaluation of the algorithms is carried out by using the modified Åström-Jury-Agniel algorithm given in [13]. The final parameters are obtained by decision making.

D. Normal Boundary Intersection (NBI)

This method was proposed in [12] as an answer to the problems presented by the weighted sum approach. It is formulated as follows:

$$\begin{array}{ll} \text{minimize} & \xi, \quad \text{respect to } \mathbf{u} \in \mathbf{U}, \\ \text{subject to} & \boldsymbol{\Phi}\,\boldsymbol{\gamma} + \xi\;\mathbf{n} = \mathbf{J}(\mathbf{u},\boldsymbol{\alpha}) - \mathbf{J}^{\circ}\,. \end{array}$$

$\boldsymbol{\Phi} \in \mathbb{R}^{nf \times nf}$ is a pay-off matrix, in which its ith column is defined as

$$\boldsymbol{\Phi}(:,i) = \mathbf{J}(\mathbf{u}_i{}^{\circ}, \boldsymbol{\alpha}) - \mathbf{J}^{\circ}\,, \quad (31)$$

where $\mathbf{J}(\mathbf{u}_i^\circ,\boldsymbol{\alpha})$ is the vector of objective functions, which is calculated at the minimum of the ith objective function. Moreover,

$$\boldsymbol{\Phi}(i,i) = 0\,. \tag{32}$$

Since $\mathbf{u}_i^\circ$ is the minimizer of $J_i(\mathbf{u},\boldsymbol{\alpha})$ over $\mathbf{u}_j^\circ, j = 1,\cdots, nf$, it follows

$$\boldsymbol{\Phi}(j,i) \geq 0,\ j \neq i\,. \tag{33}$$

Components of vector $\boldsymbol{\gamma}$ are positive scalars satisfying $\sum_{i=1}^{nf}\gamma_i = 1$. The quasi-normal vector $\mathbf{n}$ is defined as

$$\mathbf{n} = -\boldsymbol{\Phi}\mathbf{e}, \tag{34}$$

where $\mathbf{e}\in\mathbb{R}^{nf}$ is a column vector of ones in the criterion space. Since each component of $\boldsymbol{\Phi}$ is positive, the negative sign guarantees that $\mathbf{n}$ points to the origin of the criterion space. Thus, NBI has the property that a solution point is independent of how the objective functions are scaled for any $\boldsymbol{\gamma}$. As $\boldsymbol{\gamma}$ is continuously modified, the solution presents a nearly uniform distribution of Pareto optimal points representing the complete Pareto set.

The NBI method may also yield non-Pareto optimal points. Therefore, it does not provide a sufficient condition for Pareto optimality but this cannot necessarily be seen as a drawback, since such points facilitate obtaining a smoother approximation of the Pareto boundary ([12]). On the other hand, the method overlooks some Pareto optimal points, when $nf > 2$, which cannot always used as a necessary condition for Pareto optimality. However, such points tend to lie near the periphery of the Pareto set and in general are not significant. Thus, its main advantages are a Pareto front with equal spaced distributed points and the relative slow computational burden.

E. Decision making

All points that belong to the Pareto front are solutions of the multi-objective optimization problem. Since only a solution has to be found, a *decision maker* has to be included. The most common decision maker chooses the Compromise Solution (CS) as the final one, i.e. the solution with minimum distance to the utopia point.

Another way is to use *bargaining games* ([22]). This kind of games yields a practical technique for selecting a unique point from the Pareto front (see Fig. 1). In the following four bargaining games are described as decision makers. the *Nash* solution of the game (*NS*) corresponds to a point of the Pareto set which yields the largest rectangle (*c*, *B, NS, A*), the *Kalai-Smorodinsky* solution (*KS*) is situated at the intersection of the Pareto front and the straight line, which connects the threat point and the utopia point, and the *egalitarian* solution (*ES*) yields the point given by the intersection of the Pareto front and a 45°-line through the threat point. In the current work, solutions yielded by bargaining games are studied.

F. Parameters initialization

The evaluation of the performance indices requires that all roots of the characteristic polynomial of the closed loop system have negative real part (i.e. the closed loop system has to be stable). However, this fact does not guarantee the stability in the case of an interval polynomial system, which has to satisfy the Kharitonov's stability conditions (see e.g. [11]). Therefore, a stability test according to the Kharitonov's theorem is included as constraint in the optimization procedure.

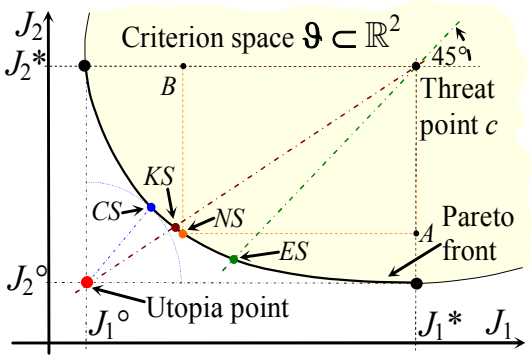

Fig. 1. Different criteria for the decision making

Moreover, the search procedure can take a very long time or it could not converge at all, if possible solutions are always taken from a subspace in the parameter space, which yield an unstable closed-loop system. In [16], a procedure for finding out the set of all stabilizing PID controllers is proposed but no mechanism for selecting a unique controller from this set is given. This allows searching in the stabilizing parameter subspace saving time and guarantying a stable final solution. However, this procedure cannot be used in the current work due to several reasons: *i*) it is based in the stability condition for single transfer functions and the formulation here is given for an interval polynomial; *ii*) an ideal PID controller is used (i.e. $P(s) = s$) while here a real controller is considered, and an additional parameter (p_1) has to be included in the optimization process, and *iii*) the stabilizing parameter subspace results to be convex, but this is not necessary the case when the system is modelled by interval polynomial.

Thus, an extensive search procedure is introduced in the present work based, which checks the Kharitonov's stability conditions in order to determine the stabilizing parameter subspace. This finally depicted in a 3D graphic (q_0, q_1, q_2), which is parameterized in p_1 (see Fig. 5 for an example). Hence, the search algorithm has to determine first the next value for p_1 in order to select the subspace in which 3-tuples (q_0, q_1, q_2) will be selected.

III. Reverse Osmosis Desalination System

A. Experimental plant

The reverse osmosis plant considered here is a very small plant for high purification of tap water. Therefore, it has no energy recovery device and no post-treatment stage is necessary. The conductivity of permeate is adjusted by mixing the product with a small amount of feed water (i.e. tap water). Permeate flow rate is controlled by a valve at the exit of retentate stream. The plant has been designed for a normal operation with a valve opening of 100% and a nominal pressure of 16 bars. In order to avoid damages in the membranes the valve should not be completely closed for a long time. For a valve opening of 10% the pressure increases up to 20 bars with the pump's temperature increasing between three and five degrees. They are still very safe values of pressure and temperature. Thus, the safe valve's excursion is 10-100%. Notice that all these characteristics are proper of this kind

of plants. Plants for sea water desalination have completely different design and safety operation conditions, where pressure values of 80 bars are normal and a post-treatment stage is essential.

The laboratory plant consists basically of a vertical centrifugal high pressure pump, an active carbon filter, a security cartridge filter and three membranes assemblies. The plant supplies in nominal operation 250 l/h permeate with a conductivity value of 7 µS/cm for 500 l/h feed water at 800 µS/cm. The schematic diagram of Fig. 2 shows the placement of sensors and actuators as well as the serial/parallel configuration of the pressure vessels.

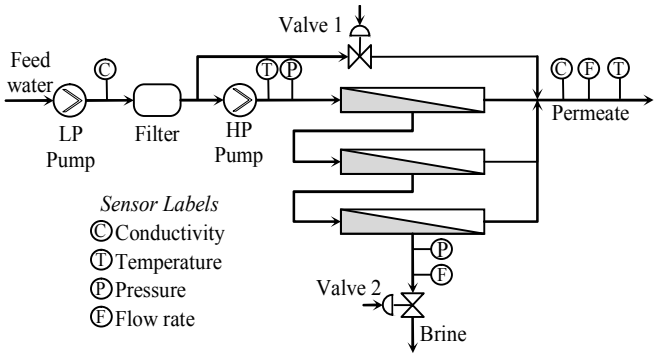

Fig. 2. Schematic representation of the RO plant

B. Dynamic Characteristics of the Plant

Normally, two inputs and two outputs are defined for this kind of RO desalination plants, namely flow rate and concentration value (sometimes also the conductivity) of permeate as outputs and the transmembrane pressure and bypass flow rate.

For this study, the plant is however simplified to a SISO system, where the input is the valve position (Valve 2) that manipulates the brine flow rate and the output the permeate flow rate. The valve on the bypass pipeline (Valve 1) is maintained closed all the time.

The operating point was set at 250 l/h permeate flow rate for a 50% of valve opening. As it was mentioned in the introduction, it very difficult to obtain a unique constant model of the plant because the membrane permeability changes very often due to changes in the feed water temperature (this is typical when the pump becomes warmer) fouling and scaling. System identification several times after-before cleaning using the N4SID algorithm ([19]) yields different models, which can be summarized as interval polynomials denoted by

$$A^{\#}(s)y(s) = B^{\#}(s)u(s) \tag{35}$$

where $A^{\#}(s)$ and $B^{\#}(s)$ are given by

$$B^{\#}(s) = [-139.26, -131.77]s + [-56.51, -47.35] \tag{36}$$

and

$$A^{\#}(s) = s^3 + [0.71, 0.96]s^2 + [0.112, 0.635]s + [0.003, 0.071]. \tag{37}$$

A nominal model is randomly obtained and presented for information but later it is not used for the controller design. This nominal model is

$$B(s) = [-134.3615\,s - 49.414] \tag{38}$$

and

$$A(s) = s^3 + 0.8157s^2 + 0.3274s + 0.0492\,. \tag{39}$$

The model before the cleaning is called "*lower model*" and the model after cleaning will be the "*upper model*". These models are not constant between several cleaning cycles and therefore parameters should be updated after two or three cycles.

Dynamic properties obtained by analyzing the models are shown in Fig. 3. Notice that lower and upper models have very different pole-zero maps, where the real pole of the lower model is dominant. Moreover, step responses are negative for positive steps, i.e. a positive step moves Valve 2 in the opening direction increasing the retentate flow rate and consequently decreasing the permeate flow rate. The settling time for the lower model is about 30s while for the upper model 20s.

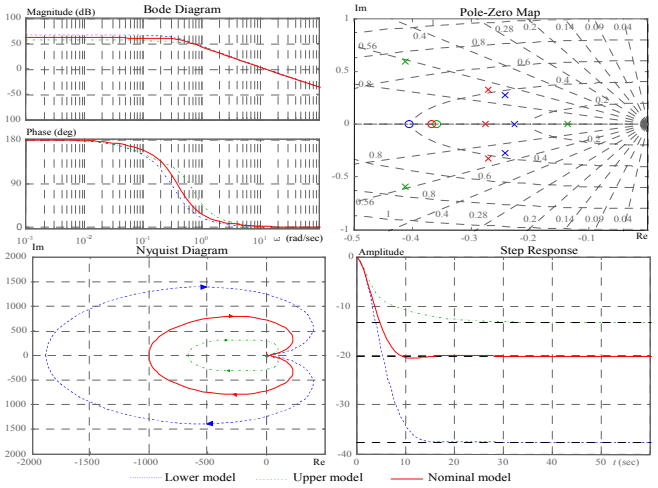

Fig. 3. Process characteristics for models before and after cleaning as well as nominal model

IV. Controller Design For the RO Process

The procedure for the controller design described in Section 2 is used for the plant presented in Section 3. The corresponding closed-loop system is shown in Fig. 4, where the PID controller consists of three polynomial whose parameters are summarized in the vectors $\mathbf{q} = [q_0\ q_1\ q_2]^T$, $\mathbf{p} = [1\ p_1\ 0]^T$ and $\mathbf{t} = [t_0\ t_1\ t_2]^T$, with $t_2 = q_2$.

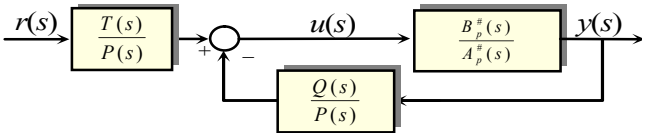

Fig. 4. Close-loop system with modified PID controller

The first activity is to determine the stabilizing subspace in the parameter space for the model given in the form of interval polynomials of eq. (36) and (37). The result is shown in Fig. 5.

Hence, the search domain for each parameter is defined as follow:

$$-0.75 \le q_0 \le -0.12, -2.0 \le q_1 \le -0.09, -0.1 \le q_1 \le -0.02\,, \tag{40}$$

$$8 \le p_1 \le 15, -5 \le t_0 \le 5\,, \tag{41}$$

Parameter λ was chosen equal to 0.5 in order to maintain the control signal bounded under the maximum allowed value. Notice that this parameter cannot be included in the optimization process because the optimizer will produce at the end a value as close as possible to zero.

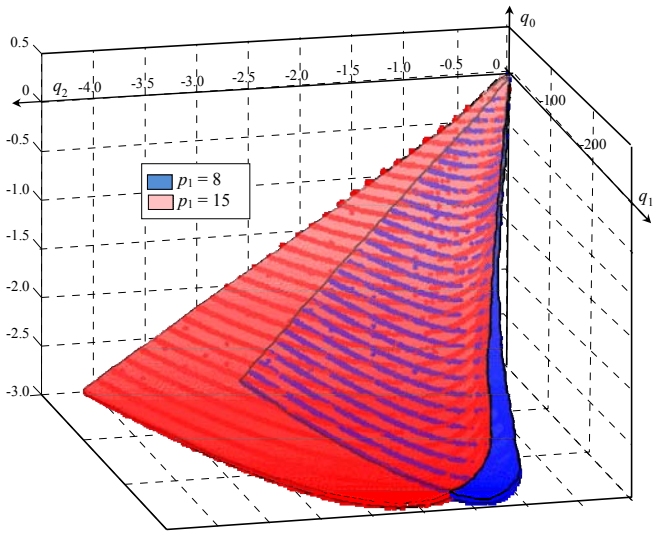

Fig. 5. Stabilizing subspace in the parameter space

Parameters are now computed by using the ISTSE as well as the ISTSC performance indices of eq. (27-29). The NBI algorithm yields the Pareto front of Fig. 6. The parameters are selected by using CS, KS, ES and NS.

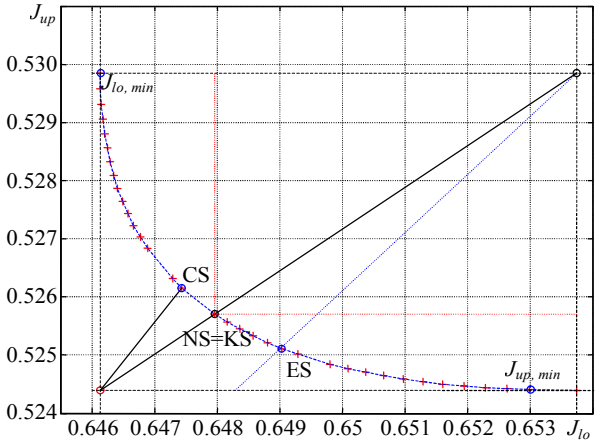

Fig. 6. Pareto front for the case ISTSE+λ ISTSC

Controller parameters and minimum values of J are summarized in Table 1. Moreover, the following performance index is used for the evaluation of the controllers during the simulation

$$J_{eval} = \int_0^{t_f} [e^2(t) + u^2(t)]\, dt\ . \qquad (42)$$

Results show that the index ISTSE yields the best performance at least for the presented example. Computation burden of the NBI algorithm is very small (6s) if it is compared with genetic algorithms (about 37 s).

Parameters obtained by using different decision makers are considered and the compromise solution is selected because of its best performance.

V. Simulation Results

The approach described above has been studied in a simulation environment. The operating point was set to 250 l/h for a valve opening of 50%. At this point, the flow rate and the valve opening are assumed to be zero. Hence the reference is changed to 285 l/h (i.e. 35 l/h over the set point) and after 20 second the set point is changed again to the value of 270 l/h (20 l/h regarding the operating point). This experiment is carried out considering the optimal controller obtained by the NBI algorithm and for the simulation three different models are used: the lower and upper models as well as an additional model obtained randomly in the parameter intervals. The simulation result is shown in Fig. 7. As it is possible to observe the controller performs satisfactory for all three models.

TABLE 1. Results for Different Parameter Sets

	ISTSE + λ ISTSC		
	CS	***Lower controller & upper model***	***Upper controller & lower model***
J^{o}_{lo}	0.5261	0.524	0.5298
J^{o}_{up}	0.6474	0.6537	0.646
J_{eval}	**994.1**	1114.6	1029.4
q_0	- 0.17	- 0.164	-0.18
q_1	- 0.217	- 0.231	-0.221
q_2	- 0.0055	- 0.0045	-0.0071
p_1	6.7310	7.241	5.354
t_0	0.00985	0.0121	0.0082
t_1	- 0.2187	- 0.2187	-0.225
t_2	-0.0055	-0.0043	-0.0071

The second study consists in analyzing the behavior of the controllers obtained for the absolute minimums, i.e. $J_{lo,min}$ and $J_{up,min}$. In order to simplify Fig. 8, the model obtained in the random way is not considered in this case. Performances can be compared by using eq. (42) (5th row in Table 1).

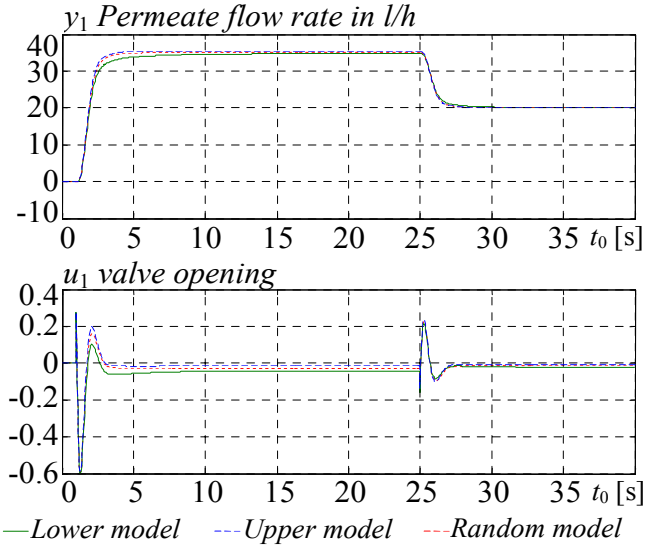

Fig. 7. Permeate flow rate and control signals for the optimal PID controller and several models of the plant

Fig. 8 shows that controllers, which are optimized for a particular model, do not perform correctly in the case of model mismatch. The controller designed by using multiobjective optimization as an optimal compromise for a family of models performs better in particular in the presence of model mismatch.

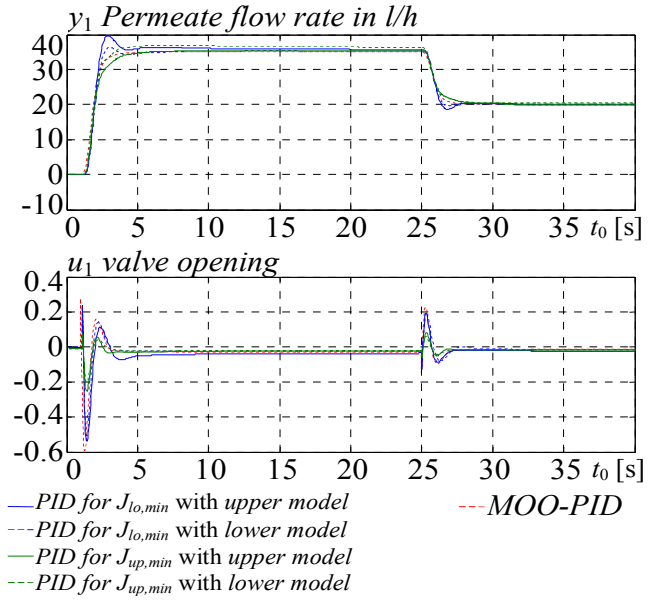

Fig. 8. Example of mismatch between controller and model used for the design

VI. Conclusions

In this work, the control problem of a reverse osmosis desalination plant, whose parameters are uncertain is solved by using the multi-objective NBI algorithm without to have to modify neither the hardware nor the software. From the practical experience, it is observed that the plant can be modeled by means of interval polynomials.

For the design, a practical version of the controller is used. This leads to a general form of controllers given by the polynomials (Q T P). The stabilizing region in the parameter space is computed by searching systematically the controller's parameters and verifying the stability condition of Kharitonov. This result is applied in order to accelerate the search of the optimization algorithm.

The simulation results shown the good performance of the controller for several plants, which are randomly chosen in the region defined by the intervals. The next step is the implementation in real-time.

References

[1] Abbas, A, Model predictive control of a reverse osmosis desalination unit. *Desalination*, **194**, 268.280, 2006.

[2] Alatiqi I., H. Ettouney, H. El-Dessouky, Process control in water desalination industry: an overview. *Desalination*, **126**, 15-32, 1999.

[3] Alatiqi, I., A. Ghabris, and S. Ebrahim. Measurement and control in reverse osmosis desalination. *Desalination*, **75**, 119–140, 1989.

[4] Al-Bastaki, N. M. and A. Abbas, Modeling an industrial reverse osmosis unit. *Desalination*, **126**, 33-39, 1999.

[5] Al-haj Ali, M., A. Ajbar, E. Ali and K. Alhumaizi, Robust model-based control of a tubular reverse osmosis desalination unit. *Desalination*, **255**, 129-136, 2010.

[6] Assef, J. Z., J. C. Watters, P. B. Desphande and I. M. Alatiqi, Advanced control of a reverse osmosis desalination unit. *Proc. International Desalination Association World Congress*, Vol. V, 174-188, Abu Dhabi, 1995.

[7] Åström, K. J., and T. Hagglund, Advanced PID Control. ISA - The Instrumentation, Systems, and Automation Society, 2005.

[8] Åström, K. J., and T. Wittenmark, Adaptive Control. Dover Publications, 2008.

[9] Bartman, A., A. Zhu, P. D. Christofides and Y. Cohen, Minimizing energy consumption in reverse osmosis membrane desalination using optimization-based control. *Journal of Process Control,* **20**, 1261-1269, 2010.

[10] Bartman, A., C. McFall, P. D. Christofides and Y. Cohen, Model predictive control of feed flow reversal in a reverse osmosis desalination process. *Journal of Process Control*, **19**, 433-442, 2009.

[11] Bhattacharyya, S.P. H. Chapellat, and L.H. Keel, *Robust Control, The Parametric Approach*, Prentice Hall, Upper Saddle River, 1995.

[12] Das, I. and J. Dennis, Normal-Boundary Intersection: A new method for generating Pareto optimal points in multicriteria optimization problems. *SIAM Journal on Optimization*, **8**, 631-657, 1998.

[13] Gambier, A., Optimal PID controller design using multiobjective Normal Boundary Intersection technique. Proc. of the 7th *Asian Control Conference 2009*, 1369-1374, Hong Kong, August 27-29, 2009.

[14] Gambier A. and E. Badreddin, Application of hybrid modeling and control techniques to desalination plants. *Desalination*, 152, 175-184, 2002.

[15] Gambier, A., A. Wellenreuther, and E. Badreddin. Optimal control of a reverse osmosis desalination plant using multi-objective optimization. Proceedings of the *2006 IEEE Conference on Control Applications*, 1368-1373, Munich, October 4-6, 2006.

[16] Hohenbichler, N,.All stabilizing PID controllers for time delay systems. Automatica, **45,** 2678_2684, 2009.

[17] McFall, C., P. D. Christofides, Y. Cohen and J. F. Davis, Fault-tolerant control of a reverse osmosis desalination process. Proceedings of *8th IFAC Symposium on Dynamics and Control of Process Systems,* 3, 163-168, Cancun, June 6-8, 2007.

[18] McFall, C., A. Bartman P. D. Christofides and Y. Cohen, Control of reverse osmosis desalination at high recovery. Proceedings of the *2008 American Control Conference*, 2241-2247, Seattle, June 11-13, 2008.

[19] Van Overschee, P. and B. De Moor, N4SID: Subspace algorithms for the identification of combined deterministic-stochastic systems. Automatica, **30**, 75-93, 1994.

[20] Riverol, C., and V. Pilipovik. Mathematical modeling of perfect decoupled control system and its application: A reverse osmosis desalination industrial-scale unit. *Journal of Automated Methods and Management in Chemistry*, 2005, 50-54, 2005.

[21] Robertson, M.W., J. C. Watters, P. B. Desphande, J. Z. Assef and I. M. Alatiqi, Model based control for reverse osmosis desalination processes. *Desalination*, 104, 59-68, 1996.

[22] Thomson, W., Cooperative models of bargaining. In: *Handbook of Game Theory with Economic App.*, R.J. Aumann & S. Hart (ed.), **2**, 1237-1284, Elsevier., 1994.

[23] Zhou, K. and , J. C. Doyle, *Essentials of Robust Control*. Prentice Hall, London, 1997.